Solid Freeform Fabrication 2022: Proceedings of the 33rd Annual International Solid Freeform Fabrication Symposium – An Additive Manufacturing Conference
Reviewed Paper

Effects of Fast Neutron Irradiation on the Microhardness of Inconel 625 and Inconel 718 Fabricated via Laser Powder Bed Fusion

M. Andurkar[1], V. O'Donnell[2], T. Keya[3], B. C. Prorok[3], J. Gahl[2], S. M. Thompson[*1]

[1] Alan Levin Department of Mechanical and Nuclear Engineering, Kansas State University, Manhattan, KS 66502, United States of America.

[2] University of Missouri Research Reactor (MURR), University of Missouri, Columbia, MO 65211, United States of America.

[3] Department of Materials Engineering, Auburn University, Auburn, AL 36849, United States of America.

*Corresponding author: smthompson@ksu.edu

Abstract

The demand for advanced materials in constructing next generation nuclear reactors has intensified the need to explore additive manufacturing (AM) processes as an alternate means of fabricating components. In this study, Inconel 625 (IN625) and Inconel 718 (IN718) samples fabricated using Laser Powder Bed Fusion (L-PBF) were irradiated using fast neutrons. Samples investigated included as-printed and heat-treated at either 700, 900, or 1050 ℃ for 1 hour to understand the impact of heat treatment on any neutron irradiation hardening. Wrought IN625 and IN718 samples were also inspected for experimental control. All samples were irradiated for 7 weeks resulting in a total fluence $2.74x10^{15}$ neutrons/cm^2. To quantify radiation damage, the Vickers microhardness was measured before and after fast neutron irradiation. Results show that the IN718 samples experienced less change (-2.5 to 3.24 %) in microhardness. On the other hand, IN625 samples underwent more (0.9 to 7.21%) change in microhardness post fast neutron irradiation.

Keywords: Selective Laser Melting, Nickel Superalloy, Vickers Microhardness, Radiation Embrittlement.

1. Introduction

The Generation IV International Forum (GIF) which represent ten nations was founded in 2000 to develop six reactor technologies that can shape future, next-generation nuclear reactors [1]. The technologies are based on meeting the increasing energy demands on a sustainable level by building clean, safe, and cost-effective nuclear reactors. Most of these six technologies use closed fuel cycle aiming to make maximum use of fuel resources and minimize radioactive wastes. Out of these six technologies, three are planned to be fast reactors which employs fast neutrons for fission reactions. Neutrons produced during fission reactions with energy more than 0.1 MeV are known as fast neutrons. Fast reactors employing fast neutrons can provide significant advantage over the current slow or thermal neutron ($E < 0.025$ eV) reactors [2]. In fast neutron reactors, natural uranium is burned 60 times more efficiently than a normal reactor. Natural uranium (0.7% U-235 and 99.3% U-238) is burned directly by fast neutrons without it being converted to plutonium isotopes eventually utilizing uranium at maximum level. This will help to reduce the scarcity of natural uranium all over the world. Moreover, fast reactors have smaller core and higher power density compared to normal

reactors. Even though, fast reactors are researched to provide significant advantages over current nuclear reactors, there is a shortage of commercial and research fast reactors in the USA.

To build safe, reliable structural components for high energy fast reactors, different material classes are qualified such as refractory metal alloys, Ni-based superalloys, Ti-based alloys. However, fabricating complex-shaped structural components using conventional machining methods is generally challenging due to high toughness and residual stress. To mitigate this issue, additive manufacturing (AM) technology serves as a novel, easier and more efficient way of building components. AM provides advantages over conventional machining like reduction in waste materials as AM operates on adding layers of material together to complete the final part in contrast to subtractive nature in conventional machining. Laser powder bed fusion (L-PBF) is one of the seven AM process categories specified in ASTM52900-21 [3]. LPBF process involves selective melting of material layer of 20-60 micron-thick within an enclosed setting of inert gas. Laser and powder interaction creates various byproducts like plume, spatter, powder ejecta due to surface tension and Marangoni effects [4]. Inert gas is used to efficiently carry these byproducts away from melt pool to obtain a clean and desired microstructure. It also reduces the oxidation of alloy and help preserve the chemical composition of alloy [5].

Ni-superalloys are proposed as attractive material for building components to be used in GEN IV reactors [6]. IN718 and IN625 finds extensive application in structural components in thermal and fast reactors. Although Ni-superalloys have been successfully adopted in nuclear reactors for many years, research has confirmed that they are prone to become highly radioactive due to high neutron absorption cross-section. Instead of this drawback, IN718 finds its use in building tensioning springs, fuel channel spacers. IN718 is an attractive material in nuclear industry due to its properties such as good corrosion resistance, high strength due to the formation of phases like metastable γ'' phase at lower temperature and equilibrium δ phase at higher temperatures [7].

Nickel based superalloys are recommended to be employed in GEN IV reactors [6]. IN625 possesses excellent high temperature strength, creep, and toughness. It is been recommended in fabricating control rod and reactor core applications [8]. IN625 is a solid solution strengthening alloy due to the pronounced micro-segregation of elements like Mo and Nb during solidification. IN625 is becoming more ubiquitous in various industries like aerospace, nuclear or any other industries where harsh environments are expected [9]. Conventional machining methods often face difficulties in processing IN625 components due to its high hardness, reduced machinability, and low thermal conductivity [10]. Fang et al. studied the microstructural evolution of IN625 specimens built via L-PBF subjected to different heat treatments [11]. It was found that as-built specimens possessed higher hardness due to high dislocation density arising from high thermal gradients during the L-PBF process. The microhardness values decreased when the as-built specimens were subjected to heat treatment temperatures at 870, 980, and 1150 ^{o}C for 1 hour. The samples were furnace cooled to room temperature. The heat treatment reduced the dislocation density and increased homogenization of grains. On the other hand, IN718 is a precipitation hardening nickel-based superalloy which derives its strengthening from D022-ordered γ'' (Ni_3Nb). Tucho et al. found that solution heat-treating IN718 samples (1100 ^{o}C for 1 hr) weakened the sub-grain boundaries indicating a reduction in dislocation density and micro-segregation of refractory metals like Nb and Mo. This ultimately resulted in a decrease of hardness compared to as-printed samples [12]. By performing heat treatment at different temperatures, different mechanical properties can be obtained from IN625 and IN718 alloys suitable for certain applications.

In the past, researchers have studied the effects of neutron and ion irradiation in IN718. Byun and Farrell studied the changes in tensile properties of wrought IN718 in solution-annealed (SA) and precipitation hardened (PH) conditions. They found the SA IN718 showed a threefold increase in yield strength and a decrease in ductility. On the other hand, the originally stronger PH IN718 showed minimal radiation hardening post irradiation [13]. Because of high cost, long time, and radioactivity of neutron irradiated samples, researchers turned towards using ion irradiation to simulate the neutron irradiation damage. Hunn et al. studied the three different ions (Fe, H, He) irradiation effects in wrought SA IN718. They found out all three ions irradiation induced radiation hardening due to the formation of helium bubbles [14]. However, the irradiation damage depth from ion irradiation is very limited to the thickness in scales of nanometer to micrometers. This is not sufficient for measuring damage via microhardness testing [15]. Andurkar et al. performed thermal neutron irradiation in L-PBF and wrought IN625 samples. They observed L-PBF built samples were lesser prone to detrimental radiation induced hardening compared to wrought samples [16]. Keya et al. conducted similar studies but using fast neutrons radiation in L-PBF and wrought IN625. From the preliminary results, they observed the L-PBF samples experienced both radiation induced hardening and softening for different fluence values [17]. Claudson studied the effects of neutron irradiation, with exposures exceeding (E >1 MeV), on the elevated temperature mechanical properties of wrought nickel-based and refractory metal alloys. The results showed a decrease in ductility at elevated temperatures compared to those measured at room temperature [18].

Although there have been several studies conducted on studying the irradiation effects in wrought IN718 and IN625, similar investigations in AM IN718 are scarce. There is a need of understanding on how AM built IN718 and IN625 would behave under similar radiation environment. For successful adoption of AM metals in nuclear industry, research studies can prove as an important guide on how to tailor the process parameters to obtain radiation hardening resistant component. This paper focuses on performing fast neutron irradiation on as-built, heat-treated, and wrought IN718 and IN625 samples. Vickers microhardness pre and post 5 weeks of fast neutron irradiation was performed to comprehend which sample condition was less prone to post irradiation hardening defect.

2. Methods

Gas atomized, virgin IN718 and IN625 powder with a mean particle size of 35 μm and 31.31 μm, respectively, were supplied by Carpenter Technologies. The elemental composition of Inconel 718 powder used in L-PBF in this study, following the ASTM F3055-14 standard for Additive Manufacturing Nickel Alloy (UNS N07718) with Powder Bed Fusion, is presented in Table 1. The chemical composition of Inconel 625 powder used for L-PBF process in this study adhering to ASTM Standard for Additively Manufacturing Nickel Alloy F3056-14 (21) is presented in Table 2. L-PBF Inconel 718 samples of dimensions 10 x 4 x 3 mm^3 were fabricated using a Concept Laser Mlab 100R system. The Concept Laser is equipped with a 100 W fiber laser with wavelength of 70 nm. The building process was carried out in an enclosed argon atmosphere for minimization of oxidization. Samples as shown in Fig. 1(a) were iteratively built at various process parameters and then inspected for density. Final process parameters consisting of power = 90 W, scan speed = 800 mm/s, laser diameter = 80 μm, hatch spacing = 60 μm, and layer thickness = 30 μm yielded 99.88% dense samples. For baseline purpose, wrought IN718 plate was procured from Metalmen NY, USA. The plate was manufactured as per ASTM B 670-07 (2013). Small 7.5 x 5 x 3 mm^3 samples were sectioned from the plate using wire electrical discharge machining (EDM). The chemical composition of all forms of Inconel 718 samples used in this study is indicated in Table 1. Inconel 625 cubes of 10 mm^3 dimension were additively manufactured using same Concept Laser Mlab 100R

system. The samples were printed in an enclosed argon atmosphere for minimization of oxidization. Cubes were iteratively built at various process parameters and then inspected for density. Final process parameters provided for 99.79% dense samples, these process parameters were: power = 90 W, scan speed = 800 mm/s, laser diameter = 80 µm, hatch spacing = 60 µm, and a layer thickness = 25 µm. In this study, only vertically printed IN625 sample highlighted in Fig. 1(b) was used. Inconel 625 plate (152.4 x 152.4 x 4.76 mm^3) was procured from Metalmen, NY, USA. The plate was manufactured per specification AMS5599. Small 1 x 1 x 0.5 cm samples were sectioned from the plate using wire electrical discharge machining (EDM). The chemical composition of all forms of Inconel 625 samples used in this study is indicated in Table 2.

Table 1: Elemental composition of L-PBF powder and wrought IN718 (% in weight)

% wt	Ni	Cr	Mo	Fe	Nb+Ta	Co	C	P	Ti	Al
ASTM	50-55	17-21	2.8-3.3	Bal	4.75-5.5	<1	<0.06	<0.015	0.65-1.15	0.2-0.8
L-PBF	50-55	17-21	2.8-3.3	Bal	5.22	<1	0.05	<0.015	0.75-1.15	0.3-0.7
Wrought	53.55	18.76	2.95	17.5	5.08	0.16	0.03	0.01	0.97	0.55

Table 2: Elemental composition of L-PBF powder and wrought Inconel 625 (% in weight)

% wt.	Ni	Cr	Mo	Fe	Nb+Ta	Co	C	P	S	Al	Ti	Mn
ASTM	Bal	20-23	8-10	<5.0	3.15-4.15	<1	<0.1	<0.015	<0.015	<0.4	<0.4	<0.5
L-PBF	Bal	21.59	9.0	2.95	3.55	0.03	0.04	<0.015	<0.015	0.11	0.11	<0.5
Wrought	Bal	22.36	9.0	0.72	3.32	0.8	0.03	0.009	0.005	0.08	0.3	0.18

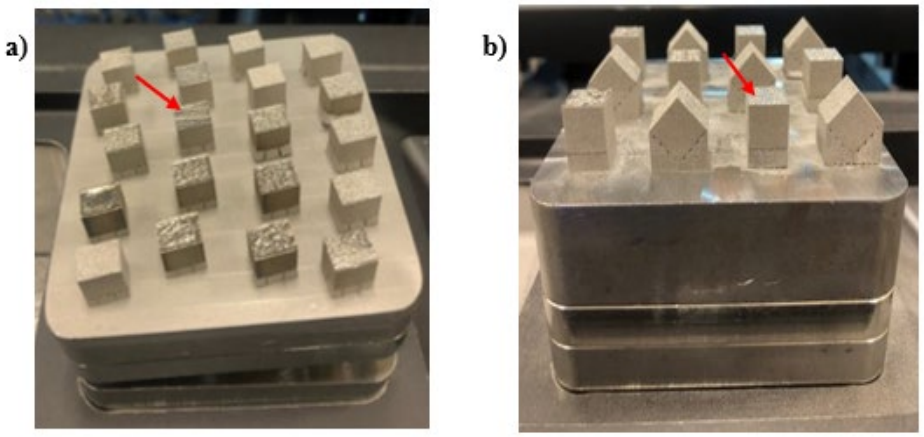

Figure 1: L-PBF built a) IN718 and b) IN625 samples. Highlighted samples indicate the optimized dense sample used in this study.

The scan strategy used in this study is island scanning strategy with a checkerboard pattern with 5 × 5 mm squares. Each island alternated the scan direction perpendicular with-respect-to adjacent islands. Samples were separated from the build plate via wire EDM and then subjected to various heat treatments. The samples were subjected to three heat-treatment

temperatures of 700, 900, and 1050 °C for 1 hour. The rationale behind selecting these temperatures was the formation of δ phase in additively manufactured IN718 and IN625 as discussed in TTT diagram in a study conducted at by R. G. Thompson and National Institute of Standards and Technology (NIST) respectively [19][20]. Wrought samples were subjected to the same heat-treatment temperatures for 40 hours. Some L-PBF specimens were not heat treated, *i.e.,* left in the as-built condition. Heating ramps used during heat treatment were ~5 ºC/min. All specimens were subjected to air cooling to room temperature while remaining in the furnace. Uncertainty in heat treatment temperatures is ± 5 ºC.

Fast neutron irradiation was carried out in cyclotron where a proton is accelerated at very high velocity using the electrically charged 'dees'. The dees are connected to oscillating current source. The dees are sandwiched between two magnets which provides magnetic force. The proton with alternative electric and magnetic force gains high acceleration. It moves in concentric circles and exits once desired acceleration is achieved. The accelerated proton was bombarded on fluorine-18 target. Once the proton is bombarded it gives off energetic neutrons as a by-product following the ^{18}O (p, n) ^{18}F reaction [21]. The process is explained schematically in Figure 2. All IN625 and IN718 samples were irradiated for a duration of 7 weeks resulting in a total neutron fluence of 2.74 x 10^{15} neutrons/cm^2.

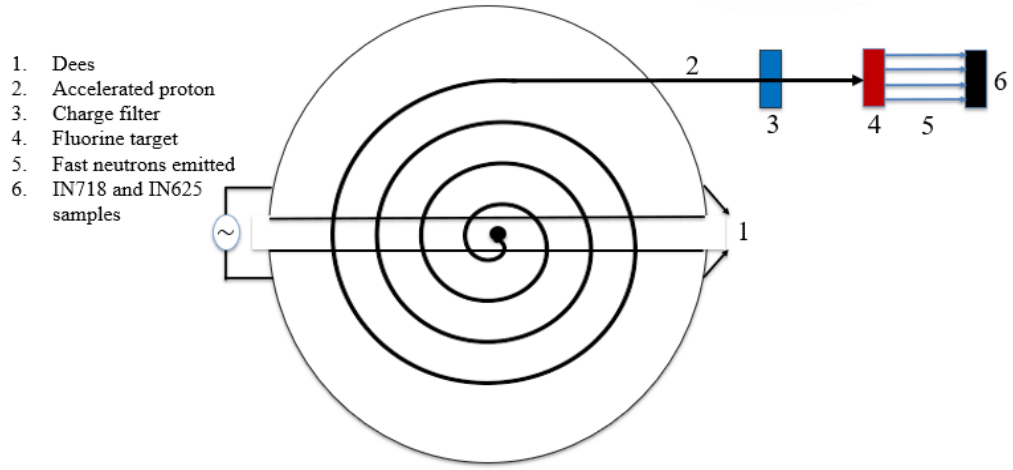

Figure 2: Schematic of fast neutrons production in cyclotron.

Hardness is an indication of yield strength. Vickers microhardness test was performed using a Phase II 900-391D microhardness tester. On each sample, 5 measurements were taken before and after irradiation to be able to calculate average and standard deviation in measurements. Error bars on the plots represent the standard deviation. The indentations were made using 1 kgf (9.8 N) load applied with a 15 secs dwell time.

3. Results

The Vickers microhardness of the pre-irradiated L-PBF as-built, heat treated and wrought IN718 and IN625 samples are shown in Fig. 3. The as-built IN718 and IN625 samples measured 326.64 $\pm$ 6.21 and 327.26 $\pm$ 9.22 HV, respectively. This indicates the process parameters used for fabricating both materials did not have a major influence on the hardness of the samples. However, the slight variation in microhardness may potentially be due to difference in chemical composition of two materials. As-built IN718 and IN625 samples showed higher microhardness compared to their as-received wrought counterparts which had a microhardness of 232.42 ± 4.19 and 244.44 ± 5.73 HV respectively. The higher microhardness in L-PBF samples may be explained by them having fine dendritic

microstructure and high dislocation densities arising from high thermal gradients present during the L-PBF process. These high thermal gradients result from very high cooling rates (~10^5 K/s) and high heat flux imposed by the laser. The high cooling and solidification rates contribute immensely to trap the heavy atoms like Molybdenum (Mo) and Niobium (Nb) along interdendritic boundaries. These heavy atoms located along sub domain boundaries restrict the sliding of dislocations under external stress which ultimately increases the hardness of the material. The lower hardness in the as-received wrought samples is due to them possessing more homogenous and equiaxed grains microstructure due to prolonged heat treatment, lesser dislocation density. Lesser segregation of heavy atoms like Mo and Nb along grain boundaries since amount of Nb in wrought samples used in this study is lesser than the L-PBF powder. Moreover, the standard deviation in hardness of wrought samples is lower compared to L-PBF samples indicating more homogenous microstructure which ultimately yields homogenous property. Post three temperatures heat treatments, the microhardness trend in both materials showed similar trend.

After the 700-1h heat treatment, the microhardness increased significantly for both materials. IN718 and IN625 measured 435.96 ± 12 HV and 353.46 ± 5.77 HV, respectively. The spike in microhardness may potentially be from the precipitation of intermetallic phase γ'' (Ni_3Nb). This precipitate impedes the motion of plastic strain caused by the Vickers indenter during the hardness testing. The increase in microhardness in IN718 post 700-1h heat treatment was significantly higher than in IN625. This is due to higher quantity of Nb and Ta in IN718 compared to that in IN625 which may result in higher precipitation of γ'' phase. Increasing the heat treatment temperature from 700 ℃ to 900 ℃ and 1050 ℃, the microhardness of both materials decreased continuously. At 900 ℃, the microhardness of IN718 and IN625 measured 347.18 ± 12 HV and 300 ± 6.6 HV respectively. Further increasing the temperature to 1050 ℃, the microhardness of IN718 and IN625 measured 277.2 ± 3.57 HV and 251.8 ± 6 HV respectively. Interestingly, L-PBF samples heat treated at 1050 ℃ reduced their hardness values and brought in the range of their as-received wrought counterparts microhardness values. The reduction in microhardness after heat treatment is possibly from elimination of dislocations, solid state transformations, grain recrystallization or grain coarsening, reduction in texture, and micro stress relaxation. Similar observations have been reported [11], [22].

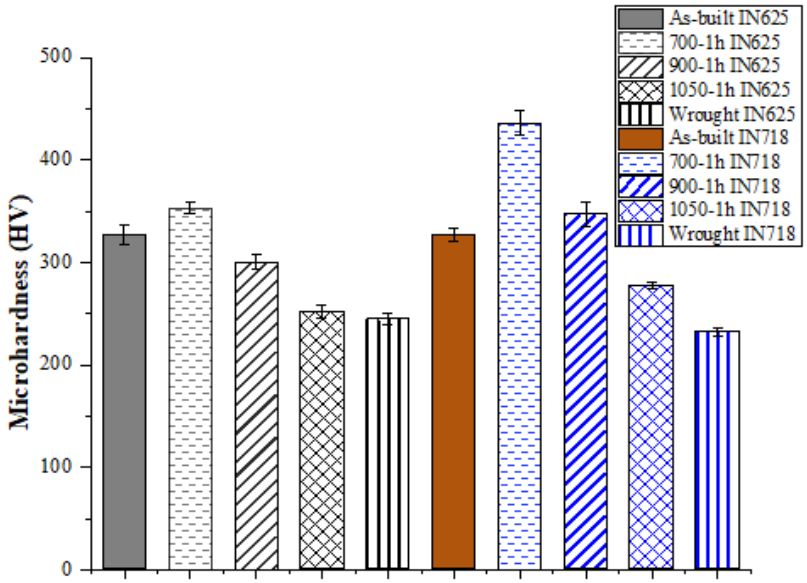

Figure 3: Microhardness of pre-irradiated as built, three heat-treated, and wrought IN625 and IN718 samples.

The microhardness values of L-PBF and wrought IN718 and IN625 samples after fast neutron irradiation are presented in Figures 4 and 5, respectively. It can be observed that fast neutron irradiation introduced radiation hardening/embrittlement in almost all samples. Helium is primarily produced in Ni-base alloys by high energy (fast) neutron reactions in natural Ni containing 68% ^{58}Ni and 26% ^{60}Ni, with the fast neutron n, α reactions. This can be explained by the neutron reaction presented in Equations (1) and (2) [23]. Helium bubbles are considered to embrittle grain boundaries by the stress developed growth of voids along the grain boundaries [8].

$$^{58}Ni + n_f \rightarrow {}^{55}Fe + {}^{4}He \quad (1)$$

$$^{60}Ni + n_f \rightarrow {}^{57}Fe + {}^{4}He \quad (2)$$

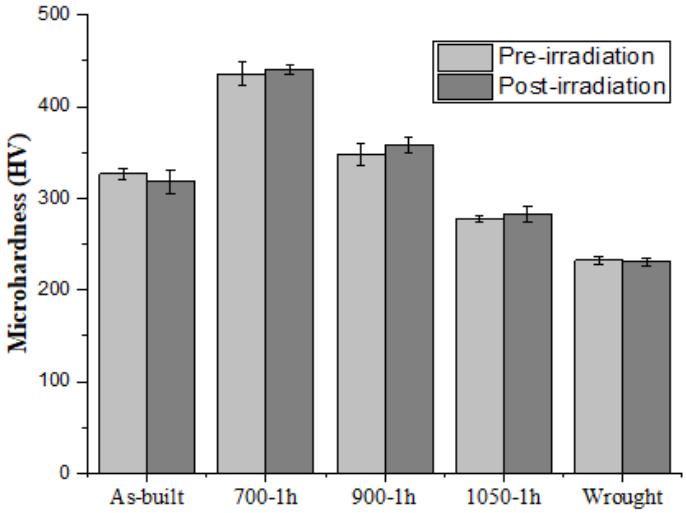

Figure 4: Pre and post fast neutron irradiation microhardness measurements of all IN718 L-PBF and wrought samples. Error bars represent standard deviation in measurements.

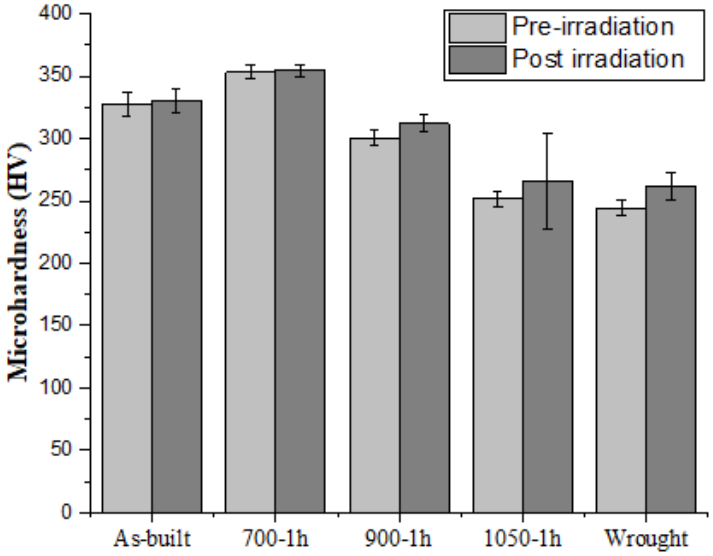

Figure 5: Pre and post fast neutron irradiation microhardness measurements of all IN625 L-PBF and wrought samples. Error bars represent standard deviation in measurements.

Although the change in hardness values in all samples is minimal post irradiation, it can result in serious damages like crack formation and ultimately result in fracture of critical end-user components. Irradiation-induced hardening was somewhat similar in all IN718 samples including wrought. This indicates that the structural integrity of AM parts under intense neutron irradiation is similar to that of conventional wrought samples. In contrast, fast neutron irradiation hardening had more influence on all IN625 samples. The percent change in microhardness post irradiation in all IN718 and IN625 samples are presented in Figure 6(a) and 6(b), respectively. IN718 was more resistant to radiation hardening possibly from the reason that IN718 have more Nb and Ta strengthening elements which could mitigate the fast neutron irradiation impact. Also, IN718 is generally known for its high strength at high temperatures compared to IN625 which is known more for corrosion resistance [24]. Similar radiation hardening or embrittlement in metals have been reported in past. [13], [25], [26].

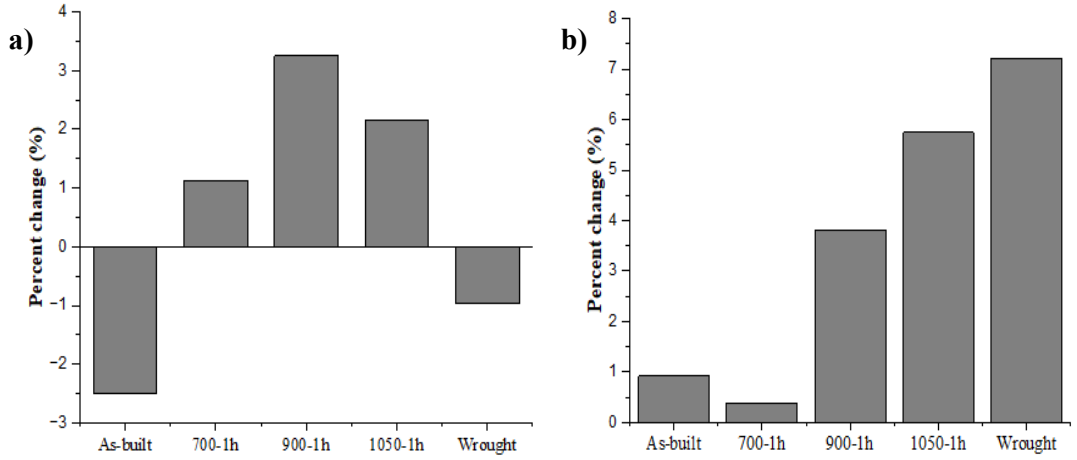

Figure 6: Percent change in microhardness of all a) IN718 and b) IN625 samples post fast neutron irradiation.

4. Conclusions

Nearly-full density IN718 and IN625 samples were fabricated using the L-PBF additive manufacturing process. The effects of fast neutron irradiation on as-built, heat-treated, and wrought conditions were studied. Vickers microhardness testing method was used to measure radiation-induced hardening in all samples. Conclusions are summarized below:

- The as-built IN718 and IN625 samples had higher pre irradiation hardness value compared to their as-received wrought counterparts.
- Post heat-treatment, both materials showed similar trend in microhardness change with increase at 700 ℃, and continuous decrease from 900 ℃ to 1050 ℃.
- Post fast neutron irradiation, all IN718 samples showed minimal percent change in microhardness ranging between -2.5 to 3.24 %.
- However, IN625 samples underwent more hardening with percent change in microhardness ranging between 0.9 to 7.21 %.
- IN718 samples displayed more resistance to radiation hardening (lower percent change) as compared to IN625 samples (higher percent change).

The results provided in this study signifies the importance of adopting accelerated testing method to emulate the irradiation effects in materials considered important in building future efficient fast reactors. The comparison of AM results along with currently used wrought

components will help boost confidence among designers/engineers to consider AM built components in future fast reactors. Fast neutron irradiation testing provides an accelerated mean of obtaining radiation effects without making materials radioactive which are difficult to handle. Different conditioned samples investigated in this study under same irradiation environment provides an insight into what condition samples performed superior to the others. The research results discussed in this study can provide assurance to certify and apply additively manufactured components in nuclear industry.

Acknowledgement

This material is based upon work supported by the U.S. Department of Energy's Office of Nuclear Energy under Award Number DE-NE0008865.

Disclaimer

References

[1] K. L. Murty and I. Charit, "Structural materials for Gen-IV nuclear reactors: Challenges and opportunities," *Journal of Nuclear Materials*, vol. 383, no. 1, pp. 189–195, 2008, doi: https://doi.org/10.1016/j.jnucmat.2008.08.044.

[2] B. Zohuri, *Generation IV nuclear reactors*. Elsevier Ltd., 2020.

[3] ISO/ASTM, "INTERNATIONAL STANDARD ISO / ASTM 52900 Additive manufacturing — General principles — Terminology," *International Organization for Standardization*, vol. 5, no. I, pp. 1–26, 2015.

[4] J. S. Weaver, D. C. Deisenroth, and S. P. Moylan, "Inert Gas Flow Speed Measurements in Laser Powder Bed Fusion Additive Manufacturing NIST Advanced Manufacturing Series 100-43 Inert Gas Flow Speed Measurements in Laser Powder Bed Fusion Additive Manufacturing," *NIST Advanced Manufacturing Series*, p. 24, 2021.

[5] F. Wirth, A. Frauchiger, K. Gutknecht, and M. Cloots, "Influence of the Inert Gas Flow on the Laser Powder Bed Fusion (LPBF) Process," 2021, pp. 192–204.

[6] A. F. Rowcliffe, L. K. Mansur, D. T. Hoelzer, and R. K. Nanstad, "Perspectives on radiation effects in nickel-base alloys for applications in advanced reactors," *Journal of Nuclear Materials*, vol. 392, no. 2, pp. 341–352, 2009, doi: 10.1016/j.jnucmat.2009.03.023.

[7] M. Sundararaman, S. Banerjee, and H. Mori, "The Stability of γ" and γ' Phases in

Alloy 718 Under Electron Irradiation," pp. 379–387, 2012, doi: 10.7449/2001/superalloys_2001_379_387.

[8] M. A. Stopher, "The effects of neutron radiation on nickel-based alloys," *Materials Science and Technology (United Kingdom)*, vol. 33, no. 5, pp. 518–536, 2017, doi: 10.1080/02670836.2016.1187334.

[9] S. Li, Q. Wei, Y. Shi, C. K. Chua, Z. Zhu, and D. Zhang, "Microstructure Characteristics of Inconel 625 Superalloy Manufactured by Selective Laser Melting," *Journal of Materials Science and Technology*, vol. 31, no. 9, pp. 946–952, 2015, doi: 10.1016/j.jmst.2014.09.020.

[10] A. K. Parida and K. Maity, "Comparison the machinability of Inconel 718, Inconel 625 and Monel 400 in hot turning operation," *Engineering Science and Technology, an International Journal*, vol. 21, no. 3, pp. 364–370, 2018, doi: 10.1016/j.jestch.2018.03.018.

[11] C. Li, R. White, X. Y. Fang, M. Weaver, and Y. B. Guo, "Microstructure evolution characteristics of Inconel 625 alloy from selective laser melting to heat treatment," *Materials Science and Engineering A*, vol. 705, no. August, pp. 20–31, 2017, doi: 10.1016/j.msea.2017.08.058.

[12] W. M. Tucho, P. Cuvillier, A. Sjolyst-Kverneland, and V. Hansen, "Microstructure and hardness studies of Inconel 718 manufactured by selective laser melting before and after solution heat treatment," *Materials Science and Engineering A*, vol. 689, no. February, pp. 220–232, 2017, doi: 10.1016/j.msea.2017.02.062.

[13] T. S. Byun and K. Farrell, "Tensile properties of Inconel 718 after low temperature neutron irradiation," *Journal of Nuclear Materials*, vol. 318, no. SUPPL, pp. 292–299, 2003, doi: 10.1016/S0022-3115(03)00006-0.

[14] J. D. Hunn, E. H. Lee, T. S. Byun, and L. K. Mansur, "Ion-irradiation-induced hardening in Inconel 718," *Journal of Nuclear Materials*, vol. 296, no. 1, pp. 203–209, 2001, doi: https://doi.org/10.1016/S0022-3115(01)00519-0.

[15] Y. Yang *et al.*, "A correlation between micro- and nano-indentation on materials irradiated by high-energy heavy ions," *Journal of Nuclear Materials*, vol. 498, pp. 129–136, 2018, doi: 10.1016/j.jnucmat.2017.10.025.

[16] M. Andurkar *et al.*, "Effects of Build Orientation and Heat Treatment on Neutron Irradiation Hardening in Inconel 625 Fabricated via Laser Powder Bed Fusion," *32nd International Solid Freeform Fabrication Symposium (SFF)*, pp. 1026–1035, 2021.

[17] T. Keya *et al.*, "Effects of Heat Treatment and Fast Neutron Irradiation on the Microstructure and Microhardness of Inconel 625 Fabricated via Laser-Powder Bed Fusion," 2021, pp. 2271–2281, [Online]. Available: https://repositories.lib.utexas.edu/handle/2152/90706.

[18] T. T. Claudson, "Effects of Neutron Irradiation on the Elevated Temperature Mechanical Properties of Nickel-Base and Refractory Metal Alloys," *Effects of Radiation on Structural Metals*, pp. 67-67–28, 2009, doi: 10.1520/stp41318s.

[19] R. G. Thompson, J. R. Dobbs, and D. E. Mayo, "Effect of Heat Treatment on Microfissuring in Alloy 718.," *Welding Journal (Miami, Fla)*, vol. 65, no. 11, 1986.

[20] M. R. Stoudt *et al.*, "The Influence of Annealing Temperature and Time on the

Formation of δ-Phase in Additively-Manufactured Inconel 625," *Metallurgical and Materials Transactions A: Physical Metallurgy and Materials Science*, vol. 49, no. 7, pp. 3028–3037, 2018, doi: 10.1007/s11661-018-4643-y.

[21] B. D. Jeffries *et al.*, "Characterization of the neutron flux during production of 18F at a medical cyclotron and evaluation of the incidental neutron spectrum for neutron damage studies," *Applied Radiation and Isotopes*, vol. 154, no. August, p. 108892, 2019, doi: 10.1016/j.apradiso.2019.108892.

[22] J. Nguejio, F. Szmytka, S. Hallais, A. Tanguy, S. Nardone, and M. Godino Martinez, "Comparison of microstructure features and mechanical properties for additive manufactured and wrought nickel alloys 625," *Materials Science and Engineering A*, vol. 764, no. July, 2019, doi: 10.1016/j.msea.2019.138214.

[23] T. M. Angeliu, J. T. Ward, and J. K. Witter, "Assessing the effects of radiation damage on Ni-base alloys for the prometheus space reactor system," *Journal of Nuclear Materials*, vol. 366, no. 1–2, pp. 223–237, 2007, doi: 10.1016/j.jnucmat.2007.01.217.

[24] S. Pratheesh Kumar, S. Elangovan, R. Mohanraj, and J. R. Ramakrishna, "A review on properties of Inconel 625 and Inconel 718 fabricated using direct energy deposition," *Materials Today: Proceedings*, vol. 46, pp. 7892–7906, 2021, doi: 10.1016/j.matpr.2021.02.566.

[25] T. S. Byun *et al.*, "Mechanical behavior of additively manufactured and wrought 316L stainless steels before and after neutron irradiation," *Journal of Nuclear Materials*, vol. 548, p. 152849, 2021, doi: 10.1016/j.jnucmat.2021.152849.

[26] Z. H. Ismail, "Effect of low dose neutron irradiation on the mechanical properties of an AIMgSi alloy," *Radiation Effects and Defects in Solids*, vol. 112, no. 4, pp. 105–110, 1990, doi: 10.1080/10420159008213036.